

Enforced One-Dimensional Photoconductivity in Core-Cladding Hexabenzocoronenes

Yaron S. Cohen,^{†‡} Shengxiong Xiao,^{†‡} Michael L. Steigerwald,^{†‡}
Colin Nuckolls,^{*†‡} and Cherie R. Kagan^{*†‡§}

Department of Chemistry, Columbia University, New York, New York 10027,
The Nanoscience Center, Columbia University, New York, New York 10027,
IBM T. J. Watson Research Center, Yorktown Heights, New York 10598

Received August 28, 2006

ABSTRACT

Photoconductivity in contorted hexabenzocoronene liquid crystals is found to be exclusively one-dimensional. Spectroscopic measurements and density functional theory support the existence of two π -systems attributed to a low-energy radialene-core and higher energy out-of-plane alkoxyphenyl rings. Persistent photocurrents, measured as a function of field, channel length, and intensity, fit a stretched exponential characteristic of intracolumnar transport, restricted through the radialene-core by the alkoxyphenyl-cladding. Bimolecular recombination is enhanced with increasing carrier concentration by the system's one-dimensionality.

Recently, we reported the synthesis of columnar liquid crystalline materials formed from the self-organization of contorted hexabenzocoronenes (HBCs) **1** (Figure 1a).¹ The molecular substructure of **1** represents the intersection and fusion of three pentacene subunits. Due to steric interactions in the periphery of this molecule, it is significantly bent away from planarity, as shown in Figure 1c. This HBC structure **1** has been shown to have relatively high carrier mobilities and current modulation ($\mu = 0.02 \text{ cm}^2 \text{ V}^{-2} \text{ s}^{-1}$; on-off current ratio of $10^6:1$) in field effect transistors made with liquid crystalline films,¹ self-assembled monolayers,² and nanostructured cables.³

In this paper, we report photocurrent measurements of **1** and discuss the role of the molecular structure on charge generation, separation/recombination, and transport in thin films of these liquid crystalline materials. We show by UV-vis spectroscopy and density functional theory (DFT) that the molecular design provides a low-energy hexaradialene-core and a higher-energy alkoxyphenyl insulating cladding (Figure 1a). Photoconductivity measurements are consistent with the core-cladding structure, restricting the absorption of visible light and the subsequent transport of separated charges to the one-dimensional liquid crystalline core.

The synthesis of the tetradodecyloxy HBC (**1**) has been previously reported.¹ We deposit thin films on quartz

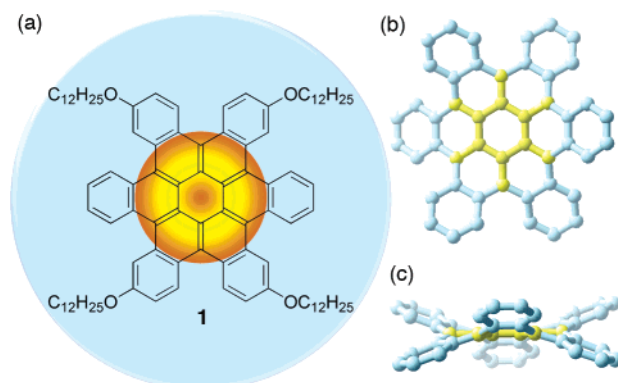


Figure 1. (a) Structure of contorted tetra(dodecyloxy)hexabenzocoronene (HBC) **1**. The hexaradialene core is highlighted in orange and the insulating cladding in blue. Crystal structure (from reference 1) showing the (b) face-on view and (c) side-on view of the compound with the hydrogens and sidechains removed to clarify the view. The low-energy hexaradialene core is shown in yellow and is surrounded by the alkoxyphenyl cladding in blue.

substrates by spin-casting⁴ and subsequently annealing at $150 \text{ }^\circ\text{C}$ for 2 h. To form the electrodes, we evaporate 2000 Å of Au through a shadow mask. These top-contact electrodes are separated by 6 to 95 μm and are between 250 and 1500 μm wide. We measure dc photoconductivity at room temperature in ambient atmosphere after subtracting device dark currents. We illuminate the devices with visible light from a 100 W Xe lamp in combination with a monochromator. Bias voltage was applied and the photocurrent measured using a source meter. A mechanical shutter

* Corresponding authors. E-mail: cheriek@us.ibm.com (C.R.K.); cn37@columbia.edu (C.N.).

[†] Department of Chemistry, Columbia University.

[‡] The Nanoscience Center, Columbia University.

[§] IBM T.J. Watson Research Center.

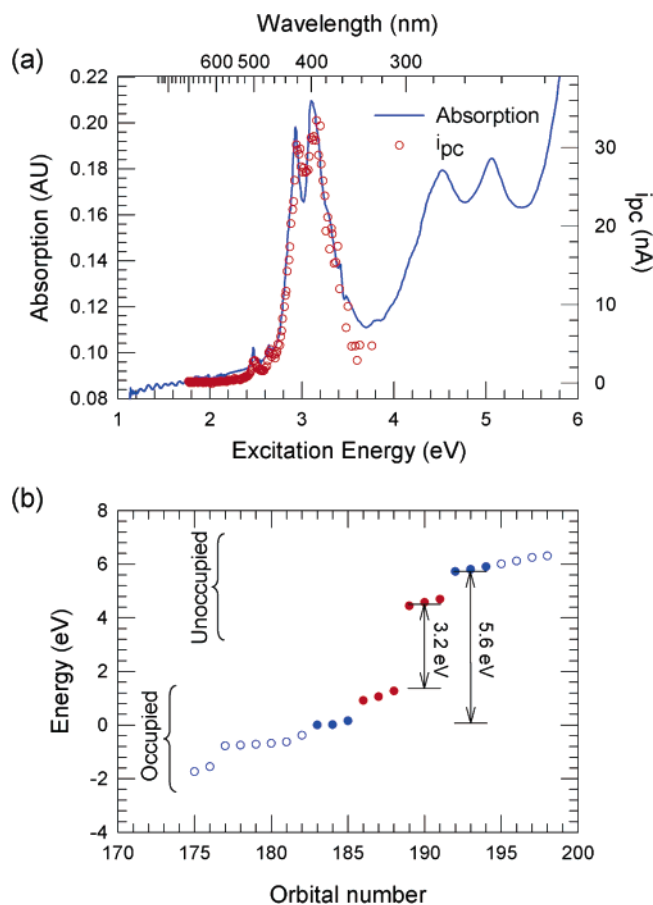


Figure 2. (a) Optical absorption spectrum (solid line) and photocurrent spectral response (circles) of tetra(dodecyloxy)-hexabenzocoronene thin films. The photoconductivity is shown for an electric field of 2.87×10^5 V/cm. (b) Molecular orbital energies of tetra(methoxy)hexabenzocoronene calculated by DFT.

was used to modulate the sample illumination and mark the start in persistent photocurrent measurements.

The optical absorption spectrum of **1** is shown in Figure 2a (solid line).⁵ The molecular geometry of **1** (Figure 1b,c) suggests that its π -space is not fully conjugated. While the central six-membered ring is close to planar, the six outer phenyl rings are significantly displaced from the plane of the central ring. As a result, the six “coronene rings” are severely distorted from planarity. This causes the “radialene” resonance structure to dominate, and only the pendent phenyl rings would be considered benzene-like. To verify this, we performed density functional theory (DFT) calculations on the tetramethoxy-substituted HBC analog of **1**. Experimental details and the frontier molecular orbitals are contained in the Supporting Information. The relative energies of the highest-energy occupied orbitals (π) and the lowest-energy unoccupied molecular orbitals (π^*) are shown in Figure 2b. The six highest-energy occupied orbitals divide into two groups, each group containing three nearly degenerate orbitals. The three higher-energy occupied orbitals (filled red circles) are located mostly on the radialene core of **1**, while the lower-energy occupied orbitals (filled blue circles) are more closely related to the surrounding phenyl rings. The three lowest-energy unoccupied orbitals (filled red circles) are related to the radialene-core and are degenerate as well,

while the higher-energy unoccupied orbitals (filled blue circles) are of mixed character. While the bifurcation is not absolute, these results support the presence of two separate π systems, one related to the radialene-core of the HBC molecule with a π - π^* energy difference of approximately 3.2 eV and the other transition related to the surrounding phenyl rings, with a π' - π'^* energy gap of approximately 5.6 eV.

In the absorption spectrum of **1**, there are three sets of peaks that merit attention: the strong absorptions at ~ 3 eV, the pair of strong absorptions centered at ~ 4.9 eV, and the comparatively weak absorptions at ~ 2.5 eV. We suggest that the peaks at 3 eV are due to the “radialene” π - π^* transition-(s). The several overlapping peaks are likely due to combinations of vibronic excitations. The 1200 cm^{-1} splitting of the two major peaks is consistent with C=C vibrations in aromatic systems. The absorptions at 4.9 eV involve the pendent phenyl rings but are difficult to assign further. The weak absorptions at 2.5 eV are most likely due to (radialene π)-(radialene π^*) triplets. These same weak transitions were seen in UV-vis of the original synthesis by Clar and co-workers of the underivatized HBC, but they were not assigned.⁶ The assignment of these transitions to a triplet state is supported by the fluorescence spectrum shown in the Supporting Information. Moreover, transition moment calculations show that the lowest-energy excitations are strongly allowed, so weak absorptions must be due to otherwise forbidden processes.

Figure 2a (open red circles) shows the photocurrent spectral response of thin films of HBC **1**. The spectral response is independent of the applied electric field and overlaps the linear absorption spectrum of the compound. The measured photocurrent originates from photoexcitations generated in the radialene-core of the compound. At fixed wavelengths, the shape of collected I-V characteristics is superlinear as the applied electric field ionizes the excitations. The shape of the I-V curve and spectral response is characteristic of photoconductivity in molecular⁷ and polymeric materials.⁸ The behavior is phenomenologically described by the modified Onsager model as photogenerated excitations rapidly relax to the lowest excited state of the compound and are subsequently separated by the applied field.⁹⁻¹¹ An important observation from the data in Figure 2a is that the efficiency of charge separation in these contorted HBCs is high, ~ 1 at electric fields $\geq 10^4$ V/cm. These materials are exciting candidates for photovoltaics because of this high efficiency.

We measured persistent photocurrents as a function of applied field and electrode separation in order to study charge transport in HBC **1** thin films. The normalized photocurrent decays are shown in Figure 3 after the device was illuminated for 7 min. The decay curves were fit to the stretched exponential:

$$i_{\text{pc}}(t) = i_0 \exp[-(t/\tau)^\beta], \quad 0 < \beta < 1 \quad (1)$$

where i_{pc} is the photocurrent and τ is the carrier lifetime. This equation is referred to as the Williams-Watts^{12,13} or

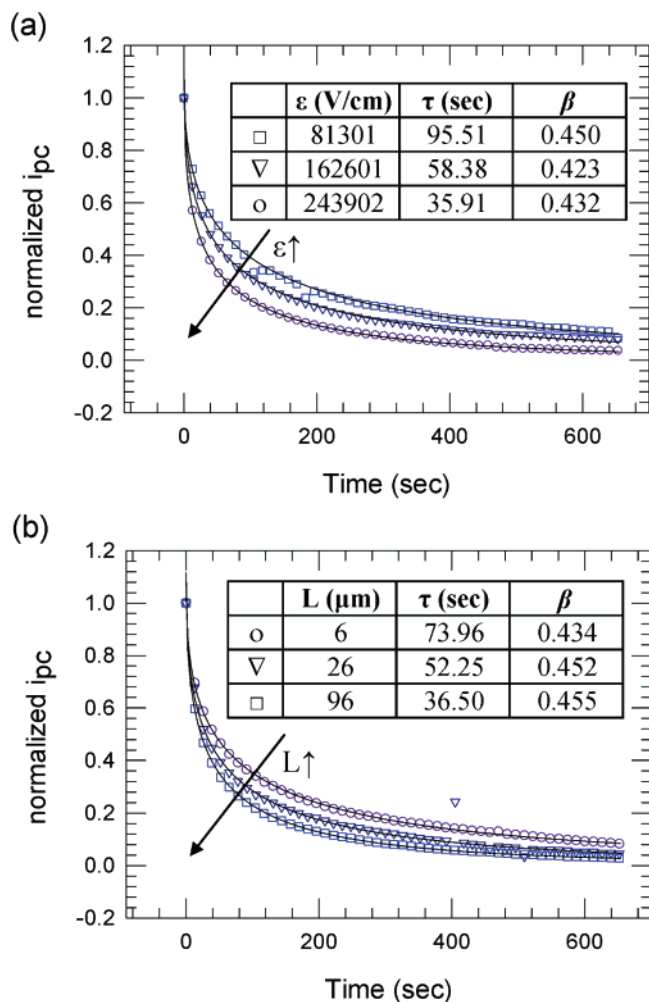


Figure 3. Persistent photocurrents of HBC **1** thin films as a function of (a) applied electric field (ϵ), at constant light intensity ($\sim 300 \mu\text{W}/\text{cm}^2$) using 2.96 eV (420 nm) excitation with a junction separation of 15 μm , and (b) electrode spacing (L) at constant light intensity ($\sim 300 \mu\text{W}/\text{cm}^2$) using 3.11 eV (400 nm) excitation and an applied field of 2.1×10^4 V/cm. The solid lines are nonlinear least-squared fits of the experimental curves to a stretched exponential (eq 1 in the text). Inset is the lifetime, τ , and exponent β for each curve.

Kohlrausch function¹⁴ and, in general, describes the relaxation of systems that are not at equilibrium.^{15,16} β is generally ascribed to the degree of dispersion in the decay kinetics, with $\beta = 1$ corresponding to no dispersion, while $\beta < 1$ points to increasing dispersion as it approaches zero.¹⁷ This exponent has been connected to the dimensionality of transport phenomena where in 3D systems $\beta = 1$ and in 1D materials $\beta = 0.5$.¹³ This analysis has been applied to persistent photoconductivity measurements of organic^{18,19} and inorganic²⁰ media. For example, in polyparaphenylenevinylene (PPV), the exponent β was found to be temperature dependent and used to describe changes in the dimensionality of polaron diffusion within the polymer chains.¹⁸ In the case of the discotic compound hexa-alkoxy-triphenylene (HAT6), the exponent was related to the phase transition of the material and the crossover from 1D to 3D carrier transport.¹⁹

The tables inset in Figure 3 summarize the charge carrier lifetime, τ , and the exponent β fit to the photocurrent decay

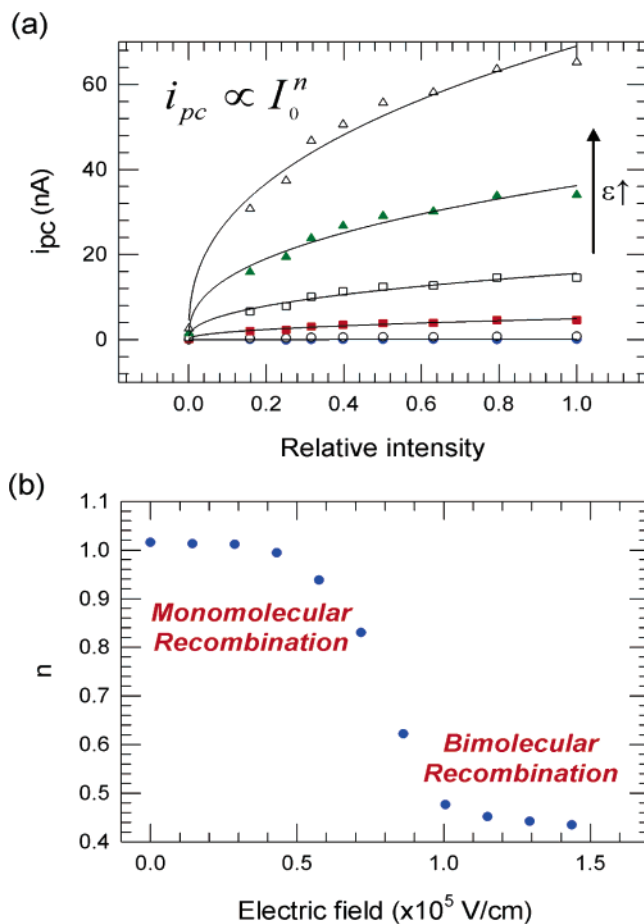


Figure 4. (a) Intensity dependence of the photocurrent for the HBC thin films at applied electric fields of (●) 0 V/cm, (○) 5.74×10^4 V/cm, (■) 1.15×10^5 V/cm, (□) 1.72×10^5 V/cm, (▲) 2.3×10^5 V/cm, and (△) 2.87×10^5 V/cm. The excitation energy was 3.1 eV (400 nm). The solid lines are nonlinear least-squared fits to $y \propto x^n$. (b) Power values, n , of the function $i_{pc} \propto I_0^n$ vs electric field.

curves. Since the time scale of the decay measurements are long (10^2 s), we assume that the decay curves probe recombination processes as well as competitive processes such as charge localization in traps or multiple trapping and detrapping processes.^{21,22} The β values of ~ 0.45 in the tables inset (Figure 3) are consistent with exclusive one-dimensional charge transport. Decay measurements for large planar disks have shown that β decreases from 0.5 to 0.2 as the length of the side chains around the core is shortened.²³ This was described by an increase in the dispersion of carrier transport as intercolumnar tunneling of carriers increases in thin films with shorter side chains. In **1** the values of β are independent of the applied electric field or device channel length, suggesting that the path of charge transport is dominated by intracolumnar transport through the one-dimensional radicalene-core. If intercolumnar transport were at all significant, the values of β would decrease with lower applied fields or with increasing electrode spacing. In **1**, the alkoxyphenyl-cladding sufficiently limits intermolecular charge transport so that only intracolumnar transport is observed.

We studied the intensity dependence of photoconductivity to probe carrier generation and recombination.²⁴ Figure 4a

shows the photocurrent versus relative intensity of 2.96 eV (400 nm) excitation at different electric fields. The photocurrent dependence on excitation intensity changes from linear to logarithmic at higher applied fields. Fitting the curves to the $i_{pc} \propto I_0^n$ reveals that the exponent $n \approx 1$ at low fields (Figure 4b), which is characteristic of monomolecular recombination.²⁵ As the applied field increases, n decreases to around 0.4, a signature of bimolecular recombination that has a square-root dependence on intensity. The transition from monomolecular to bimolecular recombination (Figure 4b) is understood by the increase in free carrier separation at higher applied fields.^{21,26} The observed bimolecular recombination is consistent with enhanced bimolecular recombination in one-dimensional semiconductors,²⁷ as the generated free carriers in HBC **1** are confined to the one-dimensional radialene-core by the alkoxyphenyl-cladding.

This study details how the self-organization of molecular substructures can encode the emergence of unique function in a material. Here the contorted HBC substructure has two mutually exclusive π -systems. The inner π -system is composed of a radialene core, which is easily excited with visible light. When stacked into supramolecular columns, the core forms a conduit for charge transport. The outer π -system provides an insulating sheath that confines the carriers to a one-dimensional path. The efficiency for charge separation is extremely high, indicating the utility of these materials in photovoltaic devices.

Acknowledgment. We thank Dr. Xuefeng Guo for enlightening discussions. We acknowledge primary financial support from the Nanoscale Science and Engineering Initiative of the National Science Foundation under NSF Award no. CHE-0117752 and by the New York State Office of Science, Technology, and Academic Research (NYSTAR) and the Department of Energy, Nanoscience Initiative (NSET no. 04ER46118). C.N. thanks National Science Foundation CAREER award (no. DMR-02-37860) and the Alfred P. Sloan Fellowship Program (2004). We thank the MRSEC Program of the National Science Foundation under award no. DMR-0213574 and by the New York State Office of Science, Technology, and Academic Research (NYSTAR) for financial support for M.L.S.

Supporting Information Available: Six occupied and six unoccupied molecular orbitals from the DFT calculations and the absorption/emission spectra from a thin film of **1**.

Also included are the experimental details for the DFT and the photoconductivity measurements. This material is available free of charge via the Internet at <http://pubs.acs.org>.

References

- (1) Xiao, S.; Myers, M.; Miao, Q.; Sanaur, S.; Pang, K.; Steigerwald, M. L.; Nuckolls, C. *Angew. Chem., Int. Ed.* **2005**, *44*, 2.
- (2) Guo, X.; Myers, M.; Xiao, S.; Lefenfeld, M.; Steiner, R.; Tulevski, G. S.; Tang, J.; Baumert, J.; Leibfarth, F.; Yardley, J. T.; Steigerwald, M. L.; Kim, P.; Nuckolls, C. *Proc. Natl. Acad. Sci. U.S.A.* **2006**, *103*, 11452.
- (3) Xiao, S.; Tang, J.; Beetz, T.; Guo, X.; Tremblay, N.; Siegrist, T.; Zhu, Y.; Steigerwald, M. L.; Nuckolls, C. *J. Am. Chem. Soc.* **2006**, *128*, 10700.
- (4) 1,2-Dichloroethane (1 mg/mL) solutions at 1200 rpm for 20 s.
- (5) The absorption of **1** is red-shifted compared to the planar HBCs that have been previously reported. See: Piris, J.; Pisula, W.; Tracz, A.; Pakula, T.; Muellen, K.; Warman, J. *Liq. Cryst.* **2004**, *31*, 993.
- (6) Clar, E.; Stephen, J. F. *Tetrahedron* **1965**, *21*, 467.
- (7) Inokuchi, H.; Maruyama, Y. In *Photoconductivity and Related Phenomena*; Mort, J., Pai, D. M., Eds.; Elsevier: New York, 1976; pp 155–184.
- (8) Gill, W. D. In *Photoconductivity and Related Phenomena*; Mort, J., Pai, D. M., Eds.; Elsevier: New York, 1976, pp 303–334.
- (9) Onsager, L. *Phys. Rev.* **1938**, *54*, 554.
- (10) Mozumdeer, A. *J. Chem. Phys.* **1974**, *60*, 4300.
- (11) Noolandi, J.; Hong, K. M. *J. Chem. Phys.* **1979**, *70*, 3230.
- (12) Williams, G.; Watts, D. C. *Trans. Faraday Soc.* **1970**, *66*, 80.
- (13) Shlesinger, M. F.; Montroll, E. W. *Proc. Natl. Acad. Sci. U.S.A.* **1984**, *81*, 1280.
- (14) Kholrausch, R. *Ann. Phys. (Liepzig)* **1847**, *12*, 393.
- (15) Palmer, R. G.; Stein, D. L.; Abrahams, E.; Anderson, P. W. *Phys. Rev. Lett.* **1984**, *53*, 958.
- (16) Chen, Y. *Phys. Rev. B* **1989**, *40*, 3437.
- (17) Warman, J. M.; Schouten, P. G.; Gelinck, G. H.; de Haas, M. P. *Chem. Phys.* **1996**, *212*, 183.
- (18) Dulieu, B.; Wery, J.; Lefrant, S.; Bullo, J. *Phys. Rev. B* **1998**, *57*, 9118.
- (19) Boden, N.; Bushby, J.; Clements, J.; Donovan, K.; Movaghar, B.; Kreouzis, T. *Phys. Rev. B* **1998**, *58*, 3063.
- (20) Kakalios, J.; Street, R. A.; Jackson, W. B. *Phys. Rev. Lett.* **1987**, *59*, 1037.
- (21) Donovan, K. J.; Elkins, J. W. P.; Wilson, E. G. *J. Phys.: Condens. Matter* **1991**, *3*, 2075.
- (22) Soci, C.; Moses, D.; Xu, Q. H.; Heeger, A. J. *Phys. Rev. B* **2005**, *72*, 245204.
- (23) Warman, J. M.; Piris, J.; Pisula, W.; Kastler, M.; Wasserfallen, D.; Mullen, K. *J. Am. Chem. Soc.* **2005**, *127*, 14257.
- (24) Leatherdale, C. A.; Kagan, C. R.; Morgan, N. Y.; Empedocles, S. A.; Kastner, M. A.; Bawendi, M. G. *Phys. Rev. B* **2000**, *62*, 2669.
- (25) Bube, R. H. *Photoconductivity of Solids*; Wiley: New York, 1960.
- (26) The impact of trapping effects is less pronounced in these intensity measurements because the illumination is continuous and the traps are expected to be filled.
- (27) Bunning, J. C.; Donovan, K. J.; Scott, K.; Somerton, M. *Phys. Rev. B* **2005**, *71*, 085412.

NL0620233